Report 1

Petro-elastic Modeling of a North Sea Field: Rock Physics Recipe and ECLIPSE Simulator *

* CIPR-PETROMAKS Project Report, 2009.

Abul Fahimuddin

Center for Integrated Petroleum Research (CIPR)
University of Bergen, Norway

Petro-elastic Modeling of a North Sea Reservoir: Rock Physics Recipe and ECLIPSE Simulator

Introduction

The reservoir characterization is the process of building a model by integration of all data available at different stages of development. The dynamic reservoir model permits us to evaluate different possible exploration scenarios [6]. During the production life of the field, history matched models are required to improve forecast reliability. For a given set of rock properties, a reservoir simulator (fluid flow modeling) provides the dynamic behaviour of fluids in place at different dates. From rock and fluid properties, it is also possible to simulate the seismic response of the saturated medium. This is the main goal of the so called petro-elastic model (PEM) or the rock physics model. A rock physics model performs the important role to link the elastic parameters which govern wave propagation, and the rock and fluid properties which govern fluid flow. The rock physics model calculates the elastic properties (e.g. acoustic impedance and Poisson's ratio) from bulk and shear modulus of mineral constituents and rock frame and also from the densities of the fluid mixture. The rock physics model is often composed of empirical laws calibrated to laboratory measurements and analytical formulas. In order to perform the fluid substitution based on Gassmann equations, we have used the forward petro-elastic recipe from Statoil ASA for a North sea field. The 3D petro-elastic model uses conventional existing rock physics models calibrated to well log data measurements. We have implemented the rock physics recipe first in Matlab and then in the Eclipse petro-elastic module [5].

From Reservoir to Seismic: Forward Modeling

The low frequency Gassmann theory predicts the resulting increase in effective bulk modulus $\mathbf{K}_{sat}$, and shear modulus $\mathbf{G}_{sat}$, of the saturated rock through the following equation:

$$\mathbf{K}_{sat} = \mathbf{K}_{dry} + \frac{(1 - \frac{\mathbf{K}_{dry}}{\mathbf{K}_s})^2}{\frac{\phi}{\mathbf{K}_{fluid}} + \frac{1-\phi}{\mathbf{K}_s} - \frac{\mathbf{K}_{dry}}{\mathbf{K}_s{}^2}}; \quad \mathbf{G}_{sat} = \mathbf{G}_{dry}, \tag{1}$$

where $\mathbf{K}$, is the effective bulk modulus with subscript referring to dry rock frame, minerals and fluid mixture. $\mathbf{G}$, is the corresponding shear modulus with different constituents and ϕ is the porosity. The effective density $\boldsymbol{\rho}_{sat}$, can be defined as a volume average of the mineral density and the fluid density. The acoustic properties of saturated porous media, e.g., isotropic compressional velocity $\mathbf{V}_P$, and shear wave velocity $\mathbf{V}_S$, can be computed as $\mathbf{V}_P = \sqrt{\frac{\mathbf{K}_{sat}+(4\mathbf{G}_{sat}/3)}{\rho_{sat}}}$, and $\mathbf{V}_S = \sqrt{\frac{\mathbf{G}_{sat}}{\rho_{sat}}}$. The acoustic impedance can be defined as $\mathbf{I}_p = \boldsymbol{\rho}_{sat}\mathbf{V}_P$. Gassmann's equation assumes a homogeneous mineral modulus and statistical isotropy of the pore space but is free of assumptions about the pore geometry. Most importantly, it is valid only at sufficiently low frequencies such that the induced pore pressures are equilibrated throughout the pore space, i.e., there is sufficient time for the pore fluid to flow and eliminate wave-induced pore pressure gradients [9]. In order to model changes in seismic response that result from fluid changes, we first need to know the initial and

target fluid properties. The effective density, $\boldsymbol{\rho}_{sat}$ may be defined as a volume average of the mineral density and the fluid density and hence, the acoustic properties of saturated porous media, e.g., isotropic compressional and shear wave velocities and acoustic impedance can be computed from these equations [1]. The effect of reservoir property changes on acoustic impedance, $\mathbf{I}_p$ has a combined response to pressure and saturation change. The polarity of the response depends on whether the pressure is increasing or decreasing and the difference between the fluid properties at the start and end of the period. Statistically, elastic properties decrease as porosity increases [12]. From lithology point of view, unconsolidated sands may have high $\mathbf{V}_p/\mathbf{V}_s$ ratio. Full saturation of a liquid in a rock increases the compressional seismic properties and shear impedance but decreases $\mathbf{V}_s$, resulting in increased $\mathbf{V}_p/\mathbf{V}_s$. Seismic properties in all rocks increase as effective pressure (difference between over-burden and pore pressures) increases [7].

ECLIPSE Petro-Elastic Model Builder

The Petro-elastic Model option in ECLIPSE [5] provides the ability to generate simulated seismic-derived quantities (such as acoustic impedance) in each active grid cell. The acoustic response of the reservoir is a combination of the acoustic responses of the different rocks and fluids that constitute the reservoir. In the Petro-elastic model, conventional simulation properties (such as pressure, fluid density, fluid saturations and effective porosity) are used to calculate the effective acoustic response of the fluids. This is then combined with the acoustic response of the rocks (both frame and minerals) to give the overall acoustic response of the reservoir. The acoustic response is calculated and output for each grid cell in the simulation model.

Effective porosity The calculation of the effective porosity, ϕ_{eff} for a grid cell is based on the porosity at the reference pressure, ϕ_0, in the grid cell and the effects of rock *compressibility* or rock *compaction*, depending on which type of pressure effect is present in the model.

Mineral bulk and shear modulus In ECLIPSE petro-elastic model, the mineral bulk modulus, $\mathbf{K}_s$ are calculated through the following polynomial function in terms of effective porosity, ϕ_{eff}:

$$\mathbf{K}_s \;=\; \mathbf{C}_0 \;+\; \mathbf{C}_1\, \phi_{\text{eff}} \tag{2}$$

Here, $\mathbf{C}_0$ and $\mathbf{C}_1$ are respectively zeroth and first order polynomial coefficient of effective porosity in calculation of the effective bulk modulus of the minerals. The mineral shear modulus is given as a direct input in the ECLIPSE data file.

Dry rock bulk and shear modulus For the dry rock frame, ECLIPSE provides a very flexible framework. We can choose any model for our choice to calculate dry rock properties; all we have to provide is a specified tabular functions of effective pressure and polynomial coefficients used to fit the dry rock properties in terms of effective porosities for each petro-elastic region [5]. When the dry frame bulk modulus, $\mathbf{K}_{dry}$ is independent of the mineral bulk modulus, it is

expressed in terms of the following polynomial regression equation in effective pressure and effective porosity:

$$(\mathbf{K}_{dry})^{\alpha} = \sum_{i=0}^{7} \{C_{\mathbf{K},i}(\mathbf{P}) \,.\, \phi_{\text{eff}}^{i}\} \\ = C_{\mathbf{K},0}(\mathbf{P}) + C_{\mathbf{K},1}(\mathbf{P}) \,.\, \phi_{\text{eff}}^{1} + C_{\mathbf{K},2}(\mathbf{P}) \,.\, \phi_{\text{eff}}^{2} + \cdots \tag{3}$$

where α is s specified constant (usually -1 or +1) and $C_{\mathbf{K},i}$ are specified tabular functions of pressure. Both α and the tabular functions are supplied directly as an input for each petro-elastic region as part of the petro-elastic model definition in the simulation model. Similar set of equations exist for the dry shear modulus:

$$(\mathbf{G}_{dry})^{\alpha} = \sum_{i=0}^{7} \{C_{\mathbf{G},i}(\mathbf{P}) \,.\, \phi_{\text{eff}}^{i}\} \\ = C_{\mathbf{G},0}(\mathbf{P}) + C_{\mathbf{G},1}(\mathbf{P}) \,.\, \phi_{\text{eff}}^{1} + C_{\mathbf{G},2}(\mathbf{P}) \,.\, \phi_{\text{eff}}^{2} + \cdots \tag{4}$$

Both α and $C_{\mathbf{G},i}$ are supplied directly as an input for each petro-elastic region as part of the petro-elastic model definition in the simulation model.

Effective Pore Fluid Properties ECLIPSE calculates the modulus and densities of each of the individual phases in every grid cell using the empirical equations given by Batzle and Wang [2]. In order to estimate the fluid bulk modulus, $\mathbf{K}_{\text{fl}}$, it uses the generalized Wood's law:

$$\frac{1}{\mathbf{K}_{\text{fl}}} = \frac{\mathbf{S}_w}{\mathbf{K}_w} + \frac{\mathbf{S}_o}{\mathbf{K}_o} + \frac{\mathbf{S}_g}{\mathbf{K}_g} \tag{5}$$

where $\mathbf{K}_{w/o/g}$ is the bulk modulus of the water/oil/gas in each of the grid cells. In addition, Eclipse provides an option to incorporate the so called *patchy saturation* concept [3].

Fluid Substitution ECLIPSE petro-elastic model exploits the standard Gassmann equation to perform the fluid substitution (see eqn. 1). Once we have found the $\mathbf{K}_{sat}$, we can calculate various seismic signatures, e.g., acoustic impedance. Eclipse uses the standard formulae to calculate seismic properties.

Link Between PEM Recipe & ECLIPSE

The present rock physics recipe of the North sea field estimates the dry rock properties from porosity and volume of clay for a given effective stress datum. The variations in elastic properties with changes in effective stress (because of changes in pore pressure) were predicted from empirical equations calibrated to velocity - stress data derived in the laboratory. The highly productive sands of this field are poorly consolidated and hence, a friable-sand or unconsolidated-line model is used to model dry rock frame [9]. In particular this rock physics model incorporates

the Hashin-Shtrikman lower and upper bounds for solid constituents [8], modified Hertz-Mindlin-Hashin-Shtrikman (HMHS) model for the dry rock properties [4], Batzle and Wang equations for pore fluid properties and Gassmann equations for fluid substitutions. The basic difference between the provided rock physics recipe and the ECLIPSE built-in PEM model lies in the calculation of the pressure corrected $\mathbf{K}_{dry}$ and $\mathbf{G}_{dry}$ modulus. Once the necessary polynomial regression coefficients, e.g., $C_{\mathbf{K},i}(\mathbf{P})$ have been calculated separately, we are ready to give these coefficients as tabular function in ECLIPSE data file.

Step 1

The rock physics recipe uses a correlation model used to calculate volume of clay from porosity: $V_{cl} = 0.7 - 1.58 * \phi$. The bulk and shear modulus of the solid phases $\mathbf{K}_s$ and $\mathbf{G}_s$ are calculated from $\mathbf{K}_{qtz}$, $\mathbf{K}_{clay}$, $\mathbf{G}_{qtz}$, $\mathbf{G}_{clay}$ and V_{cl} using the average between upper and lower Hashin-Shtrikman bounds (at 0 porosity).

$$\begin{aligned}
\mathbf{K}_{uhs} &= \mathbf{K}_{qtz} + \frac{V_{cl}}{(\mathbf{K}_{clay} - \mathbf{K}_{qtz})^{-1} + (1 - V_{cl})(\mathbf{K}_{qtz} + \frac{4}{3}\mathbf{G}_{qtz})^{-1}} \\
\mathbf{K}_{lhs} &= \mathbf{K}_{clay} + \frac{1 - V_{cl}}{(\mathbf{K}_{qtz} - \mathbf{K}_{clay})^{-1} + V_{cl}(\mathbf{K}_{clay} + \frac{4}{3}\mathbf{G}_{clay})^{-1}} \\
\mathbf{K}_s &= 0.5 * (\mathbf{K}_{uhs} + \mathbf{K}_{lhs})
\end{aligned} \tag{6}$$

$$\begin{aligned}
\mathbf{G}_{uhs} &= \mathbf{G}_{qtz} + \frac{V_{cl}}{(\mathbf{G}_{clay} - \mathbf{G}_{qtz})^{-1} + \frac{2\ (1-V_{cl})(\mathbf{K}_{qtz}+2\mathbf{G}_{qtz})}{5\ \mathbf{G}_{qtz}(\mathbf{K}_{qtz}+\frac{4}{3}\mathbf{G}_{qtz})}} \\
\mathbf{G}_{lhs} &= \mathbf{G}_{clay} + \frac{1 - V_{cl}}{(\mathbf{G}_{qtz} - \mathbf{G}_{clay})^{-1} + \frac{2\ V_{cl}(\mathbf{K}_{clay}+2\mathbf{G}_{clay})}{5\ \mathbf{G}_{clay}(\mathbf{K}_{clay}+\frac{4}{3}\mathbf{G}_{clay})}} \\
\mathbf{G}_s &= 0.5 * (\mathbf{G}_{uhs} + \mathbf{G}_{lhs})
\end{aligned} \tag{7}$$

In ECLIPSE petro-elastic model, the mineral bulk modulus are calculated through the following polynomial function in effective porosity: $\mathbf{K}_s = \mathbf{C}_0 + \mathbf{C}_1\, \phi_{\text{eff}}$, where $\mathbf{C}_0$ and $\mathbf{C}_1$ are respectively zeroth and first order coefficient of effective porosity in calculation of the effective bulk modulus of the minerals. The mineral shear modulus is given as a direct input in ECLIPSE data file. We can implement the Hashin-Shtrikman average bounds for solid phases separately from ECLIPSE and then, we can use 1st order polynomial regression fit in order to calculate the necessary coefficients $\mathbf{C}_0$ and $\mathbf{C}_1$. For a range of representative porosities, we can perform numerical calculations to get the average Hashin-Shtrikman bounds for solid phase.

Step 2

The effective pressure, $\mathbf{P}_{\text{eff}}$ in the rock physics recipe is calculated from the pore pressure ($\mathbf{P}_{pore}$) and the overburden pressure, $\mathbf{P}_{over}$. The relation that is used:

$$\begin{aligned}
\mathbf{P}_{\text{eff}} &= \mathbf{P}_{over} - \eta * \mathbf{P}_{pore} \\
\mathbf{P}_{\text{eff}} &= (-2.6 + 0.0214\ \text{TVD}) - \mathbf{P}_{pore}
\end{aligned} \tag{8}$$

here η is coefficient of internal deformation. It is common to assume η is close to one. The overburden pressure is calculated from the TVD (True Vertical Depth) from ECLIPSE. With a chosen range of representative pressure values, we can incorporate pressure corrections using Hertz-Mindlin contact theory [10] (described below: step 3) and subsequently estimate the regression coefficients, $C_{\mathbf{K},i}(\mathbf{P})$, $C_{\mathbf{G},i}(\mathbf{P})$ used in ECLIPSE input data file.

Step 3

The main effective stress and pore pressure in the porous media is explained by the Hertz-Mindlin model. In the provided rock physics recipe, the following equations are derived from Hertz-Mindlin contact theory:

$$\mathbf{K}_{HM} = \mathbf{K}_{\phi max}\left(\frac{\mathbf{P}_{\text{eff}}}{\mathbf{P}_{\text{ref}}}\right)^{\kappa} \tag{9}$$

$$\mathbf{G}_{HM} = \mathbf{G}_{\phi max}\left(\frac{\mathbf{P}_{\text{eff}}}{\mathbf{P}_{\text{ref}}}\right)^{\kappa} \tag{10}$$

Here, $\mathbf{K}_{\phi max}$ and $\mathbf{G}_{\phi max}$ are respectively high porosity bulk and shear modulus at reference pressure, $\mathbf{P}_{ref}$ and the pressure sensitivity exponent, κ is fitted to measured well log data of the North sea field at different production time. This Hertz-Mindlin equation is in accordance with the actual theoretical formulation by Dvorkin [4] but expressed in terms of reservoir-specific parameters $\mathbf{K}_{\phi max}$ and $\mathbf{G}_{\phi max}$ (explained in Table 1). In ECLIPSE petro-elastic model, there is not any concrete keyword which may implement this pressure corrections based on effective pressure. Once we have calculated the $\mathbf{K}_{HM}$ and $\mathbf{G}_{HM}$ for a set of effective pressure, we can now calculate the effective dry moduli of the solid phase for porosities below the critical porosity, ϕ_c using a modified Hashin-Shtrikman upper and lower bound iteratively.

Step 4

In the rock physics recipe, the effective dry bulk and shear modulus at the given porosity are calculated from the lower Hashin-Shtrikman bound between two end members: *zero porosity* end member has the modulus of the solid phase (calculated at step 1) and the *high porosity-pressure dependent* end member calculated in step 3. Thus the bulk modulus, $\mathbf{K}_{dry}$), shear modulus, $\mathbf{G}_{dry}$ and density, $\boldsymbol{\rho}_{dry}$ of the dry unconsolidated sand mixture are given by:

$$\mathbf{K}_{dry} = \left[\frac{\phi/\phi_c}{\mathbf{K}_{HM} + \frac{4}{3}\mathbf{G}_{HM}} + \frac{1-\phi/\phi_c}{\mathbf{K}_s + \frac{4}{3}\mathbf{G}_{HM}}\right]^{-1} - \frac{4}{3}\,\mathbf{G}_{HM} \tag{11}$$

$$\mathbf{G}_{dry} = \left[\frac{\phi/\phi_c}{\mathbf{G}_{HM} + z} + \frac{1-\phi/\phi_c}{\mathbf{G}_s + z}\right]^{-1} - z \tag{12}$$

where

$$z = \frac{\mathbf{G}_{HM}}{6}\left(\frac{9\mathbf{K}_{HM} + 8\mathbf{G}_{HM}}{\mathbf{K}_{HM} + 2\mathbf{G}_{HM})}\right).$$

The density, ρ_{dry} of the dry unconsolidated sand mixture are given by:

$$\rho_{dry} = \rho_{qtz} + V_{cl} * (\rho_{clay} - \rho_{qtz}) \tag{13}$$

In order to make both the rock physics recipe and ECLIPSE petro-elastic model comparable, we have to perform polynomial curve fitting of the calculated dry rock modulus with respect to effective porosity and effective pressure. One way of doing this is to use the modified heuristic Hashin-Shtrikman bounds for dry frame (above equations) as the input for the polynomial curve fitting. We can fit these calculated values bulk modulus values by a suitable polynomial function of the maximum order of 7 (restricted by ECLIPSE petro-elastic model). For a specified effective pressure (as explained in step 2), we can calculate a series of $\boldsymbol{K}_{dry}$ values depending on the effective porosities used all through. For example, if we use any $\mathbf{P}_{\text{eff}}$ value to calculate $\boldsymbol{K}_{HM}$ and subsequently $\boldsymbol{K}_{dry}$, we can describe the calculated polynomial regression equation of the 2^{nd} order as:

$$\begin{aligned}\mathbf{K}_{dry} &= \sum_{i=0}^{2} \{C_{K,i}(\mathbf{P}) \,.\, \phi_{\text{eff}}^{i}\} \\ &= C_{K,0}(\mathbf{P}) + C_{K,1}(\mathbf{P}) \,.\, \phi_{\text{eff}}^{1} + C_{K,2}(\mathbf{P}) \,.\, \phi_{\text{eff}}^{2}\end{aligned} \tag{14}$$

In this way we can use the rock physics recipe to calculate the necessary input, e.g., $C_{\mathbf{K},i}(\mathbf{P})$ for ECLIPSE petro-elastic model. Similarly, we can calculate the effective dry shear modulus for the frame by combining both rock physics recipe and Eclipse:

$$\begin{aligned}\mathbf{G}_{dry} &= \sum_{i=0}^{2} \{C_{\mathbf{G},i}(\mathbf{P}) \,.\, \phi_{\text{eff}}^{i}\} \\ &= C_{\mathbf{G},0}(\mathbf{P}_{\text{eff}}) + C_{\mathbf{G},1}(\mathbf{P}) \,.\, \phi_{\text{eff}}^{1} + C_{\mathbf{G},2}(\mathbf{P}) \,.\, \phi_{\text{eff}}^{2}\end{aligned} \tag{15}$$

Step 5

The modulus of the fluid mix, in the rock physics recipe, is calculated from $\mathbf{S}_w$, $\mathbf{S}_o$ and $\mathbf{S}_g$ using Wood's formula in the rock physics recipe:

$$\frac{1}{\mathbf{K}_{fl}} = \frac{\mathbf{S}_w}{\mathbf{K}_w} + \frac{\mathbf{S}_o}{\mathbf{K}_o} + \frac{\mathbf{S}_g}{\mathbf{K}_g}$$

The fluid phase density is given by:

$$\rho_f = S_w\rho_w + S_g\rho_g + S_o\rho_o$$

In ECLIPSE petro-elastic model, Wood's equation can be used as well with the proper choice of an input parameter of the keyword PECOEFS [5]. ECLIPSE also provides the scope to incorporate patchy saturation option [3].

Step 6

Once $\mathbf{K}_s$, $\mathbf{K}_{dry}$ and $\mathbf{K}_{fluid}$ have been calculated, we can use the Gassmann fluid substitution which is performed in order to predict the modulus of the saturated rock from the dry rock modulus predicted in step 4. Both the rock physics recipe and ECLIPSE petro-elastic model use the same Gassmann equation, see Eqn. (1). The fluid mixture saturation is calculated according to this equation:

$$\boldsymbol{\rho}_{sat} = \phi * \boldsymbol{\rho}_{fluid} + (1 - \phi) * \boldsymbol{\rho}_{dry} \tag{16}$$

Step 7

The elastic parameters are calculated from $\mathbf{K}_{sat}$, $\mathbf{G}_{sat}$ and $\boldsymbol{\rho}_{sat}$. Both the recipe and ECLIPSE petro-elastic model use the same equations in order to calculate elastic properties for saturated rock samples:

P-wave velocity, $\mathbf{V}_P = \sqrt{\frac{\mathbf{K}_{sat}+(4\mathbf{G}_{sat}/3)}{\boldsymbol{\rho}_{sat}}}$ S-wave velocity, $\mathbf{V}_S = \sqrt{\frac{\mathbf{G}_{sat}}{\boldsymbol{\rho}_{sat}}}$

Acoustic Impedance, $\mathbf{I}_P = \boldsymbol{\rho}_{sat}\mathbf{V}_P$ Poisson's ratio, $\mathbf{PR} = \frac{V_P^2-2V_S^2}{2V_P^2-V_S^2}$

An increase in $\mathbf{I}_P$ generally indicates that an oil reservoir is drained by water and a decrease of Poisso's ratio refers to the increase of gas saturation. But these conclusions are not trivial and hence, other factors must be considered for the proper interpretation from the saturated seismic properties.

Rock Physics Model Example in ECLIPSE

The important reservoir properties for the North sea field is shown in Table 1. We have used these parameters in the framework of rock physics formulation based on the combined recipe and ECLIPSE petro-elastic model.

Parameter Name	**Value from Statoil**
Mineral bulk mod. of quartz, $\mathbf{K}_{qtz}$	37
Mineral shear mod. of quartz, $\mathbf{G}_{qtz}$	44
Mineral bulk mod. of clay, $\mathbf{K}_{clay}$	14.9
Mineral shear mod. of clay, $\mathbf{G}_{clay}$	1.95
High porosity end member, ϕ_{max}	0.4
Reference pressure, $\mathbf{P}_{ref}$	8.8 MPa
High porosity bulk mod. at $\mathbf{P}_{ref}$	3.31
High porosity shear mod. at $\mathbf{P}_{ref}$	2.84
Pressure sensitivity exponent, k	0.233
Salinity	43000 in ppm
Temperature, T^{o}C	72

Table 1: North sea reservoir properties (modulus in GPa)

The North sea reservoir quality is generally very good with porosities in the range of 30%-35%. For the input porosity field, we have used a representative porosity distribution for a sandstone reservoir with porosity values between 0 and 0.3. The volume fraction, V_{cl} of the this field has been calculated in accordance to the empirical relation with porosity (step 1).

Solid Properties

We have used the Hashin-Shtrikman bounds for the solid phases and calculate $\mathbf{K}_s$ and $\mathbf{G}_s$. The distance between the upper and lower bounds depends on the differences in

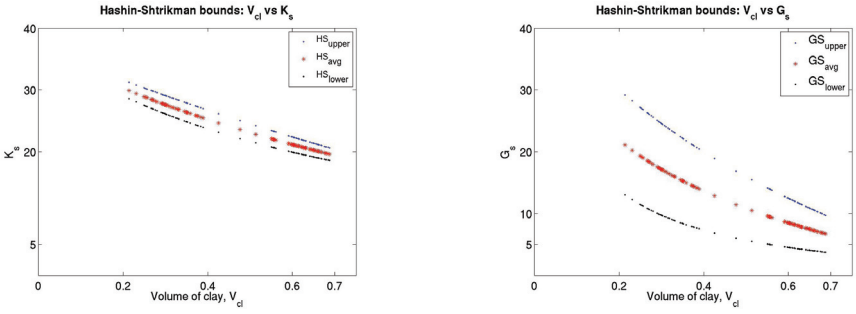

(a) $\mathbf{K}_s$ (GPa) (b) $\mathbf{G}_s$ (GPa)

Figure 1: Hashin-Shtrikman bounds for solids (in terms of V_{cl})

elastic moduli for the constituents. Widely spaced bounds can be seen for the Shear modulus when mixing sand and clay. Whereas for the bulk modulus the bounds a quite narrow as we mix sand and clay which has similar values of bulk modulus. Figure 1 shows the variation of $\mathbf{K}_s$ and $\mathbf{G}_s$ with respect to volume of clay contents

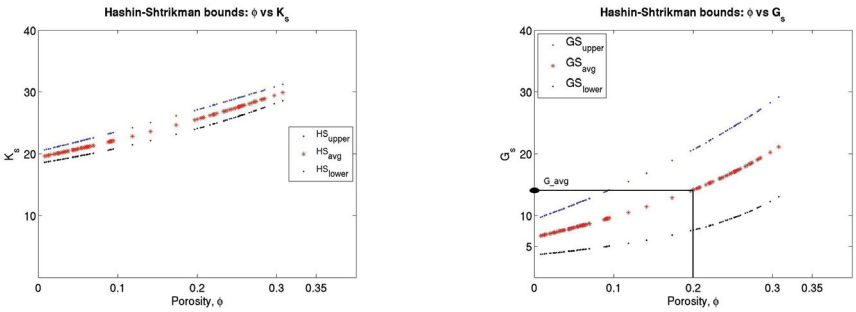

(a) $\mathbf{K}_s$ (GPa) (b) $\mathbf{G}_s$ (GPa)

Figure 2: Hashin-Shtrikman bounds for solids (in terms of ϕ)

and Figure 2 explains this variation in terms of porosity. As expected, the solid bulk modulus values increase as the porosity increases; in case of clay content, the inverse effect is observed.

If we perform 1st order polynomial fit of these $\mathbf{K}_s$ values in terms of porosities, we calculate the zeroth and 1^{st} order coefficients for ECLIPSE input: $\mathbf{C}_1$ = 33.0626 GPa and $\mathbf{C}_0$ = 19.0851 GPa (Fig. 3). For the input $\mathbf{G}_s$ in Eclipse, we have chosen an

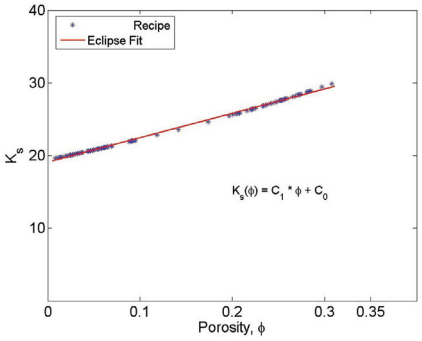

Figure 3: Polynomial Fit of $\mathbf{K}_s$ for rock physics recipe and ECLIPSE

average value of porosity as 0.2 and the corresponding $\mathbf{G}_s$ value is obtained from the average Hashin-Shtrikman curve $\mathbf{G}_{avg}$ which is approximately equal to 15 GPa (Fig. 2b).

ECLIPSE Keyword for Solids

Based on information provided in the rock physics recipe and the before mentioned combined recipe-ECLIPSE formulations, we can describe the ECLIPSE input parameters for the keyword PECOEFS [5] as

Salinity	**T**	ρ_{min}	$\mathbf{C}_1$	$\mathbf{C}_0$	$\mathbf{C}_K$	$\mathbf{C}_G$	$\mathbf{G}_s$	α	**e**	**Brie**
43000	72	2650	330626	190851	0	0	150000	1	1	0

Table 2: PECOEFS in ECLIPSE data file (Coefficients in Barsa)

Dry Frame Properties

In order to incorporate pressure effect on dry frame modulus, we have chosen a range of representative pore pressure values starting from 100 Barsa to 350 Barsa. Thus we have this set of values for pore pressure: $\mathbf{P}_{pore}$ = 100, 150, 200, 250, 300, 350 Barsa. In our case, the reference reservoir TVD value is equal to 1900 m. With these values defined, we have computed the corresponding effective pressures, $\mathbf{P}_{\text{eff}}$. For each of these $\mathbf{P}_{\text{eff}}$, we have performed the pressure corrections based on StatoilHydro recipe. Thus we have calculated pressure dependent $\mathbf{K}_{dry}$ and $\mathbf{G}_{dry}$ using both modified heuristic lower Hashin-Shtrikman bounds and Hertz-Mindlin contact theory.

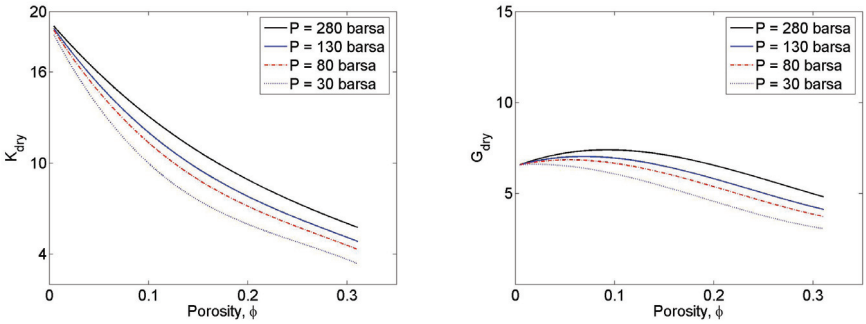

(a) $\mathbf{K}_{dry}$ (GPa) (b) $\mathbf{G}_{dry}$ (GPa)

Figure 4: Pressure dependent dry frame modulus

Figure 4 illustrates the modified Hashin-Shtrikman lower bound curves at varying confining pressure for unconsolidated sand. In figure 5(a), the $\mathbf{K}_{dry}$ values increase alongside the increased effective pressure. Also the variation of the dry frame bulk modulus is inversely proportional to the porosity for each of the different effective pressure value. In case for the dry shear modulus, we see higher $\mathbf{G}_{dry}$ values for increased effective pressure. Now for each of the effective pressure values, we can fit both the $\mathbf{K}_{dry}$ and $\mathbf{G}_{dry}$ with respect to porosity and in this way we can calculate the tabular pressure dependent coefficient values $C_{\mathbf{K},i}(\mathbf{P})$ and $C_{\mathbf{G},i}(\mathbf{P})$ for the ECLIPSE input data file.

ECLIPSE Bulk Modulus Table: PEKTABx

We have used 3^{rd} order polynomial to fit $\mathbf{K}_{dry}$ and ϕ values as follows:

$$\mathbf{K}_{dry} = \sum_{i=0}^{3} \{\mathbf{C}_{\mathbf{K},i}\,(\mathbf{P}_{\text{eff}}) \,.\, \phi_{\text{eff}}^{i}\}$$

For an illustration, at 1900 m over-burden pressure, $\mathbf{P}_{over}$ = 380.06 Barsa and thus with a varying pore pressure, we have a set of effective pressure values such as $\mathbf{P}_{\text{eff}}$ = 280, 230, 180, 130, 80, 30 Barsa. Now we perform *step* 3 and *step* 4 sequentially and then employ 3^{rd} order polynomial fit in order to calculate the necessary coefficient, $C_{\mathbf{K},i}(\mathbf{P})$ at a specific $\mathbf{P}_{\text{eff}}$. In order to check how good is our polynomial fit, we have chosen two extreme values of $\mathbf{P}_{\text{eff}}$ such as 280 and 30 Barsa. Figure 5(a) illustrates the curve fit for $\mathbf{P}_{\text{eff}}$. Similar trends are observed for other effective pressure values as well. At this point we can tabulate all the polynomial coefficient values for each of the $\mathbf{P}_{\text{eff}}$ values. Here the units for the $C_{\mathbf{K},i}(\mathbf{P})$ values are in Barsa (standard in ECLIPSE).

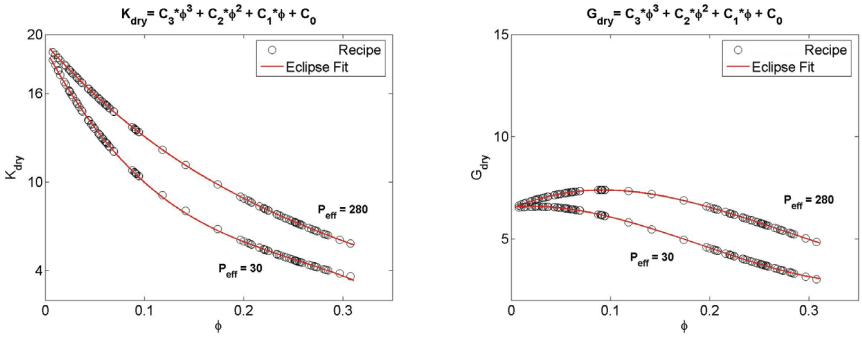

(a) $\mathbf{K}_{dry}$ (GPa) (b) $\mathbf{G}_{dry}$ (GPa)

Figure 5: Comparing Rock physics Recipe and ECLIPSE: $\mathbf{K}_{dry}$ & $\mathbf{G}_{dry}$

ECLIPSE Shear Modulus Table: PEGTABx

We have used 3^{rd} order polynomial to fit $\mathbf{G}_{dry}$ and ϕ values as follows:

$$\mathbf{G}_{dry} = \sum_{i=0}^{3} \{\mathbf{C}_{\mathbf{G},i}\,(\mathbf{P}_{\text{eff}}) \cdot \phi_{\text{eff}}^{i}\}$$

With the previously specified $\mathbf{P}_{\text{eff}}$ values, Now we perform *step* 3 and *step* 4 first for dry shear modulus and then employ 3^{rd} order polynomial fit in order to calculate the necessary coefficient, $C_{\mathbf{G},i}(\mathbf{P})$ at any specific $\mathbf{P}_{\text{eff}}$ value. In order to check the goodness of the polynomial fit, we have chosen two extreme values of $\mathbf{P}_{\text{eff}}$ such as 280 and 30 Barsa. Figure 5(b) illustrates the curve fit for $\mathbf{P}_{\text{eff}}$ in the case of $\mathbf{G}_{dry}$. Similar trends are observed for other effective pressure values as well. At this point we can tabulate all the polynomial coefficient values for each of the $\mathbf{P}_{\text{eff}}$ values. Here the units for the $C_{\mathbf{G},i}(\mathbf{P})$ values are in Barsa.

Synthetic Example of Saturated Elastic Properties

In our example we have used Archie's formula [11] to calculate a realistic water saturation profile based on standard resistivity log parameter values. The Archie equation takes the following form:

$$\mathbf{S}_w^n = \frac{a}{\phi^m} * \frac{\mathbf{R}_w}{\mathbf{R}_t}$$

Where, $\mathbf{S}_w$ is water saturation, n is the saturation exponent, resistivity of the formation fluid, $\mathbf{R}_w$, rock resistivity of the possible hydrocarbon, $\mathbf{R}_t$, cementation factor, m and a constant value, a. In our case, we have used: a=1, $\mathbf{R}_w$ =1, $\mathbf{R}_t$ =265, n =2.9 and m =1.14. The calculated water saturation profile is displayed in the Fig. 6.

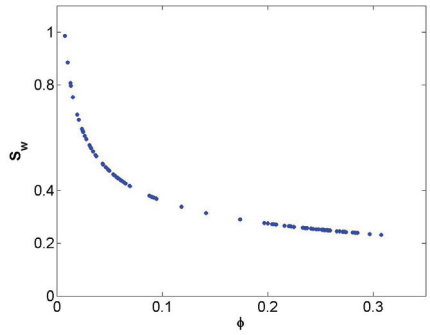

Figure 6: Representative Water saturation profile

Pore Fluid Properties

We have used the Batzle and Wang empirical relationships for brine, oil and gas in order to calculate the fluid mixture bulk modulus and density. For example, in case of $\mathbf{P}_{\text{eff}}$ = 280 Barsa, we have found these fluid mixture bulk modulus values for each of the different types of fluid: $\mathbf{K}_w$ =2.197, $\mathbf{K}_g$ =2.523 and $\mathbf{K}_o$ =3.04 GPa. Then, we have used the Wood's formula to find the effective fluid bulk modulus, $\mathbf{K}_{\text{fl}}$. The water saturation, $\mathbf{S}_w$ is being calculated using Archie formula and we have considered the case when we have only oil, the gas saturation considered to be zero.

Pressure Dependent saturated Elastic Properties: No Gas

At this point, we have measured the effective solid properties based on the rock physics recipe using Hashin-Shtrikman average bounds, $\mathbf{K}_s$, pressure dependent dry frame modulus by Hertz-Mindlin based modified Hashin-Shtrikman lower bounds, $\mathbf{K}_{dry}$ and the effective pore fluid properties, $\mathbf{K}_{\text{fl}}$ by Batzle and Wang empirical relationships. Thus, we can use the Gassmann fluid substitution formula (eqn. 1) to

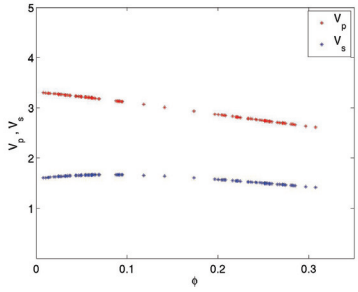

(a) $\mathbf{V}_P$, $\mathbf{V}_S$ (Km/s)

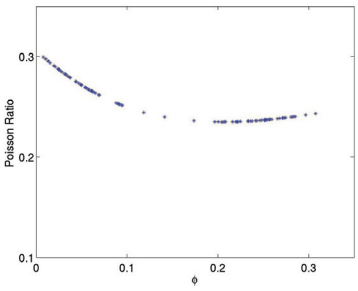

(b) Posson's ratio

Figure 7: Saturated Seismic Signatures Vs. Porosity

predict the saturated synthetic elastic properties for the field at different effective pressure. In this case, we have used $\mathbf{P}_{\text{eff}} = 30$ Barsa. We have also calculated the saturated compressional and shear velocities, $\mathbf{V}_P$, $\mathbf{V}_S$ and poisson's ratio, **PR** for a given water saturation profile (Fig. 6). We have plotted these elastic properties against the porosity values in the Fig. 7. Also we have reported the variation of seismic velocities with respect to water and oil saturation (Fig. 8). From Fig. 7a, it is evident

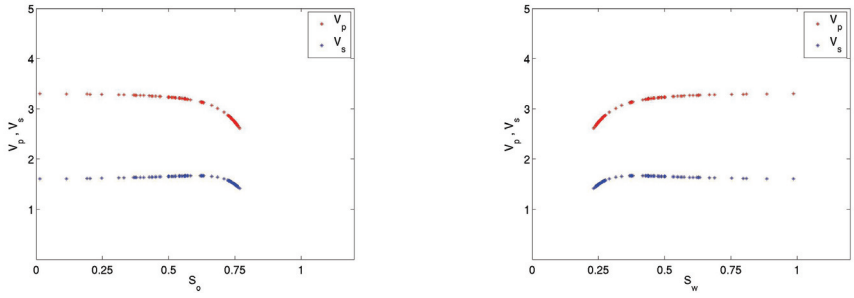

(a) Oil Saturation (b) Water Saturation

Figure 8: Saturated Seismic Signatures Vs. Saturation

that the both compressional and shear seismic velocities decrease with increased porosity which is the characteristic V-shape trend for a sandstone reservoir in the North sea [1]. Also $\mathbf{V}_P > \mathbf{V}_S$ and this is the trend along the porosity variation. Fig. 7b describes the Poisson's ratio variation with respect to porosity. With increased porosity, the value of Poisson's ratio decrease for a specific effective pressure. Also as water replaces oil, the Poisson's ratio is increased at a later situation where we have higher water saturation values (Fig. 8b). With a increased oil saturation values, there is decrease of seismic velocities and this effect can be observed from the Figure 8(a). An opposite situation prevails when oil is replaced by water. Fig. 8b shows the effect of increased water saturation on the seismic velocities.

Discussion & Comments

In this work, we have calculated synthetic seismic signatures based on a rock physics recipe. In addition, we have implemented this recipe in ECLIPSE-PEM module. The goal of this report is to implement the rock physics model so that we can integrate this PEM modeule in our overall 4D seismic history matching framework.

Bibliography

[1] Avseth P, Mukerji T, and Mavko G, *Qualitative seismic interpretation: Applying rock physics tools to reduce interpretation risk*. Cambridge University Press, 2005.

[2] Batzle M, Wang Z, *Seismic properties of pore fluids*, Geophysics Prospecting, vol. 57, (1992).

[3] Brie A, Pampuri F, Marsala AF, Meazza O, *Shear sonic interpretation in gas-bearing sands*, SPE Annual Technical Conference and Exhibition, Dallas, Texas, (1995).

[4] Dvorkin J and Nur A, *Elasticity of high-porosity sandstones: Theory for two North sea data sets*, Geophysics, vol. 61, (1996).

[5] ECLIPSE, *Eclepse Technical Description*. Schlumberger - GeoQuest, 2007.

[6] Gosselin O, van de Berg S, Cominelli A, *Integrated history matching of production and seismic data*, SPE Annual Technical Conference and Exhibition, New Orleans, Louisiana, (2001).

[7] Hansen H, Gommesen L, Ouair Y El, *Using RFT data for elastic rock properties' dependency on pore pressure in 4D quantitative analysis*, SPE Europec/EAGE Annual Conference & Exhibition, Vienna, Austria, (2006).

[8] Hashin Z and Shtrikman S, *A variational approach to the elastic behavior of multi-phase materials*, Journal of Mech. Phys. Solids, vol. 11, (1963).

[9] Mavko G, Mukerji T, and Dvorkin J, *The rock physics handbook: Tools for seismic analysis in porous media*. Cambridge University Press, 2003.

[10] Mindlin R, *Compliance of elastic bodies in contact*, Journal of Appl. Mech., vol. 16, (1949).

[11] Rider M, *The geological interpretation of well logs (second edition)*. Rider-French Consulting Ltd, 2002.

[12] Wang Zee, *Fundamentals of seismic rock physics*, Geophysics, vol. 66, NO.2, (2001).